Charged Particle Effects on Optoelectronic Devices and Bit Error Rate Measurements on 400 Mbps Fiber Based Data Links

Paul Marshall[1,2], Cheryl Dale[1], and Ken LaBel[3]

1 Naval Research Laboratory, Washington, DC, 20375
2 SFA, Inc., Landover, MD, 20785
3 NASA Goddard, Greenbelt, MD, 20771

Abstract

Proton test results on a fiber optic data link operating at 400 megabits/s (Mbps) are described to elucidate the roles of important variables such as proton angle of entry and the optical signal strength. Interpretation of these data reveals that direct ionization events from protons can result in bit errors, though these effects can be mitigated with increased optical signal strength. We explore the consequences of these results to suggest single event tolerant approaches for satellite applications, and conclude that radiation tolerant links and busses can operate in even the most severe orbital environments with acceptable error rates of $< 10^{-9}$.

I. Introduction

The maturity and improved reliability of fiber optic data transmission methods now make this technology available for satellite designers to take advantage of the high date throughput and low noise and power characteristics. Presently, reliable fiber optic data bus architectures exist for satellite telemetry and control applications at 1 Mbps [1], and developments are under way for payload data busses operating at rates approaching 1 Gbps. It is crucial that performance be maintained in the presence of the space radiation environment which includes total ionizing dose and single particle effects which can disrupt link performance.

Indications are that fiber based data links can be made to operate with little degradation or interference in the earth's trapped radiation belts [2,3]. Reference [3] examines the results of extensive radiation testing and flight data for the NASA Small Explorer Data System (SEDS) MIL-STD-1773 telemetry and control bus which operates at rates up to 1 Mbps. This bus relies on system level error handling to maintain performance in the presence of single event effects (SEE). Point-to-point link investigations at data rates of 37 and 138 Mbps have also been conducted in the presence of protons [4]. These tests indicate good total dose and transient behavior for the LED-based 1300 nm components tested.

In this paper, we extend the investigation of SEEs to data rates of 400 Mbps and analyze experiments in which operating fiber bus components are subjected to proton bombardment. We then examine variables such as proton energy, proton flux, angle of incidence, data rate, and optical signal level. Parameterization of bit error rate (BER) effects in terms of these variables offers insights into the physical mechanisms involved, and suggests both circuit modification and device selection criteria to maximize link performance. By combining predicted trapped particle orbital environmental data, including spacecraft shielding effects, with system response under test, we outline an approach to predict BER in orbit and use this as a basis for evaluating proposed hardening solutions. Proton test issues, including beam dosimetry and time structure, are also discussed as they affect data integrity.

II. Experimental Details

A. Single Event Measurement

Since previous investigations [3,4] had indicated SEE susceptibility from ionization in photodetectors, we choose an InGaAs photodiode, the Epitaxx ETX 75 p-i-n diode, which has an active optical diameter of 75 μm. Our analysis has indicated better SEE characteristics for III-V direct bandgap detectors since the depletion depth need only be about 2 μm for >80% quantum efficiency. In contrast with indirect bandgap detectors such as Si for 850 nm applications in which depletion depth are about 20 times larger, the thin structure should minimize both the "target" size for ion strikes as well as the ion pathlength when hit. Moreover, this device is characteristic of the design choices being considered for high bandwidth data busses since the thin junction provides minimal capacitance.

A commercial bit error rate test (BERT) set from Broadband Communications Products, Inc. was configured to measure of link performance as shown in figure 1. The tester was set to generate a serial pseudorandom numeric (PN) sequence of (2^7-1) bits in length. No encoding algorithms were exercised though this relatively short sequence length provides a reasonable approximation of bit patterns found in schemes such as 8B/10B encoding. The rate of 400 Mbps was established by an internal oscillator within the test set. Data from the sequence generator were provided to the 1300 nm laser source which coupled light into a 9 μm core single-mode fiber. The fiber link included an air-gap attenuator so that the desired optical power level could be adjusted over the range of -30 dBm to -9dBm. The optical power was monitored by an external lightwave meter or coupled onto the surface of the photodiode under test. Light was launched onto the photodiode using a 3-axis

micro-manipulator stage, and coupling efficiency was maximized by tuning and monitoring the photodiode output on a digital sampling oscilloscope.

Photodiode irradiation took place without exposing any associated circuitry. This was possible because the trans-impedance preamplifier was offset about 1 cm so it could be shielded from the proton beam. The electrical amplifier output was returned to the BERT where clock recovery and PN pattern recognition were performed. Test set output included the BER as well as the number of errors and the error free intervals down to 0.01 s. With no protons incident, a BER of 10^{-9} was measured with -27 dBm incident on the photodiode. We note that this matches the theoretical limit for the bipolar trans-impedance amplifier arrangement (gain=1000, 80% quantum efficiency, and 400 Mbps), and confirms that we had accurate measurement of the incident optical power to the photodiode.

With protons incident on the photodiode, we monitored the BER and the number of errors. Measurements of BER were typically made with > 100 total errors to assure good statistics. This usually covered a time interval of minutes, and the error free interval feature provided information to assure that we were monitoring individual events and not contiguous errors from a single strike.

B. Dosimetry and Beam Structure

Tests were performed at the Crocker Nuclear Laboratory Cyclotron Facility at the University of California at Davis. Proton beam energies are tunable at selected energies over the range from 8 to 67 MeV. The beamline developed by the Naval Research Laboratory for radiation effects testing has been described previously[5]. The dosimetry measurement uses a 5-foil secondary emission monitor calibrated against a Faraday cup. Ta scattering foils located several meters upstream of the target establish a beam spatial uniformity of 15% over a 2 cm radius circular area. This results in some energy loss. For example, the 67 MeV internal tune is degraded to 63 MeV as it passes through the scattering foil, the beamline exit window, and 10 cm air to reach the device under test. Beam currents from about 5 pA to 50 nA allow testing with proton fluxes from 10^6 to 10^{11} protons/cm^2/s. Beam control commands and dosimetry are facilitated via computer control.

The beam temporal structure follows from the 22 MHz cyclotron frequency (at 67 MeV) and provides micro-pulses of approximately 1.3 ns duration every 44 ns. This structure has particular importance for high data rate in-situ tests since, as in this case, a serial bit period of 2.5 ns is only slightly longer that the micro-pulse. Furthermore, only about 1 in 35 bit periods coincide with the arrival of protons on the detector! Strict analysis would dictate careful consideration of the beam flux during the micro-pulse as well as the probability of a bit coinciding with a pulse rather than assuming an average beam flux incident during all bit intervals. Fortunately, these two approaches yield the same result *provided* the bit error rate is independent of beam flux.

Our tests examined the error cross-section as a function of beam flux to assure independence and therefore simplify this analysis. For single bit errors, this implies that we stay below the regime where frequent multiple particle events occur. However, if one measures message interrupts from one or more words (such as with MIL-STD-1773), the beam flux must stay low enough to prevent 2 bit errors in the same *message* so that this does not become an issue [3]. Always, one must carefully consider the beam temporal structure and its relation to the data stream when conducting high data rate in-situ tests.

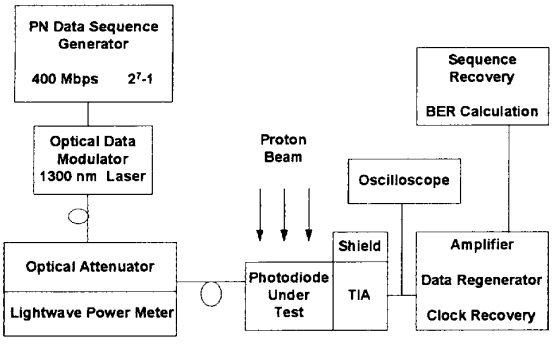

Figure 1. The proton-induced bit error rate test arrangement focused on the photodetector where the electrical signal is smallest and the particle effects are most pronounced.

III. Results and Discussion

A. Proton Cross-section Measurements

Proton-induced BER effects can be quantified according to the well-developed tools used in more conventional SEE investigations. Bit error rate cross-sections represent the ratio of failed bits to the particle fluence incident on the device during the interval in which the failures were measured. Unlike static memory upsets however, the cross-section dependence on particle flux must be considered, as previously discussed. Here, we saw no flux dependence. Also, the measured cross-section has been shown to depend linearly on the transmitted data rate in the NASA SEDS bus [3]. We have not yet performed such tests, but we do expect a data rate BER dependence. Likewise, the proton energy dependence must be considered especially since we have determined that direct ionization from protons, without nuclear reaction events, are responsible for SEEs in the photodiode [3,4,6]. In this case, there is no lower proton energy threshold, and the cross-

section decreases slightly with increasing proton energy. Other important aspects include the particle angle of incidence as well as the circuit level and system level issues which ultimately govern the effects of a given particle event.

The test circuit and transmission scheme depicted in figure 1 closely replicates the type of NRZ asynchronous data transmission approach being considered for satellites. The test configuration includes provisions for characterizing SEEs throughout (and well beyond) the optical power level envelope expected for typical optical power budgets for either ring or star bus architectures. Experience has highlighted the need for such application-specific test approaches [7].

To quantify the effects of proton induced bit errors and the dependence on system parameters, we present BER cross-sections versus receiver optical power in figure 2. Comparison of the top two curves of the figure illustrates the effect of the incident angle. The proton trajectory with respect to the right circular cylinder effectively establishes the proton pathlength and therefore the amount of charge deposited by direct ionization. For the 75 μm diameter by 2 μm thick geometry corresponding to the ETX-75, the maximum pathlength is 75 μm, across the diameter. This corresponds to 90 degree incidence shown in the figure.

Both the magnitude and optical power dependence of the two cross-section curves reveal insights into the SEE characteristics. At -25 dBm, near the maximum sensitivity of the detector, we note that the cross-section magnitude is about 10^{-6} cm^2. Calculating the projected area of the diode in the beam at 90 degrees, we note that it too is about 10^{-6} cm^2. The fact that the measured and physical cross-sections agree so closely confirms that, under these conditions, essentially all incident particles can result in a bit error. This is highlighted by the fact that the 50 degree tilt, which increases the projected area, actually increases the BER above that seen with the 90 degree position even though the pathlength of protons through the device can be no more than about 3 μm. By increasing the optical power, the link is made less sensitive to bit errors. This occurs for both orientations in the beam, but at an accelerated rate with the 50 degree tilt. Since randomly arriving protons in satellites would seldom be co-aligned with the diode's plane, we note that the 50 degree curve should be more typical of expected flight dependence. This suggests that system designers can use optical power as a means to affect the link performance in the presence of protons.

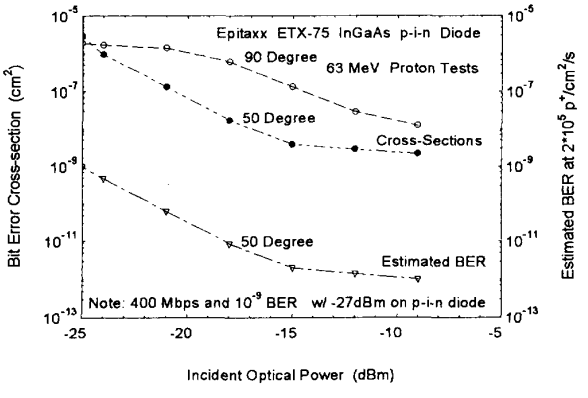

Figure 2. The top curves indicate bit error cross-section dependence on the receiver incident optical power for 63 MeV protons incident at 90 degrees, in the plane of the planar diode, and when tilted 50 degrees. The lower curve estimates BER when subjected to a proton flux from a large solar flare such as the 1972 King flare.

B. Ion Interactions

As charged particles such as protons traverse semiconductor materials, Coulomb excitation of valence electrons results in ionization tracks, which in depleted regions of a photodiode, undergo charge separation with the charge collected in the circuit. The magnitude of this charge depends on several factors including the ion path length and the ion's linear energy transfer (LET). The LET, in turn, depends on the ion species and its energy as well as the particular semiconductor material and its density. Figure 3 illustrates this situation for the case of the spectrum of proton energies expected in a 2600 km circular orbit behind 150 mils of Al shielding. The figure shows the number of electron-hole pairs collected per micron of proton path length in the $In_{0.53}Ga_{0.47}As$ material used for 1300 nm lightwave detection. Note that the lower energy protons are more abundant and more heavily ionizing. The charge liberated in the 1 μm path by the lower energy protons

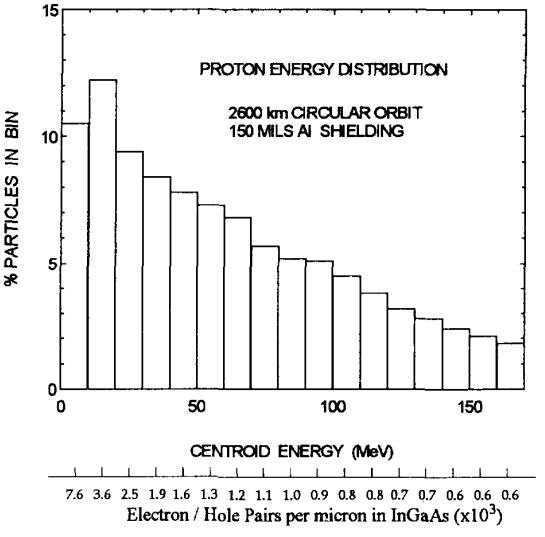

Figure 3. This typical shielded proton spectrum is binned to reveal an abundance of lower energy protons. The lower scale shows that thousands of electrons are freed per micron path length in the InGaAs photodiode.

approaches that which would be sensed as the optical signal for a bit period for a link operating at 400 Mbps with an optical power level of about -27 dBm.

In addition to the direct ionization by the charged particle, collisions and reactions can occur which cause lattice atoms to recoil and produce further ionization along with lattice displacement damage. For protons below about 8 MeV, the interactions are via the repulsive Coulomb force and result in recoil atoms with energies of several hundred eV. As the proton energy increases, it can overcome the Coulomb barrier, and nuclear elastic scattering results in more energetic, and more heavily ionizing recoils which can dislodge other atoms and may deposit tens of keV of ionization energy. For protons above 20 MeV, nuclear reactions become increasingly important. In this case, the lower energy Coulomb collisions are hundreds of times more likely, but very energetic reaction-induced recoils are also possible resulting in several MeVs of ionization energy deposited in a small region. These large ionization events give rise to single event upset (SEU) in microelectronic circuits and may cause bit errors in fiber link photodetectors. The cross-sections for these various reactions are proton energy dependent as well as material dependent.

C. On-Orbit Performance Estimates

Drawing on the accepted models of the radiation environments and the interaction mechanisms described in the previous section, it is now possible to evaluate the probability of having an ionization event of a given magnitude in a satellite environment. Referring to the outline shown in figure 4, we rely on the NASA and NRL environment models (AP-8 for protons and CREME for cosmic rays), and any of several accepted shielding/transport codes to evaluate the particle environment reaching the device of interest. The particle environment is represented in an energy dependent and time dependent manner for each particle species.

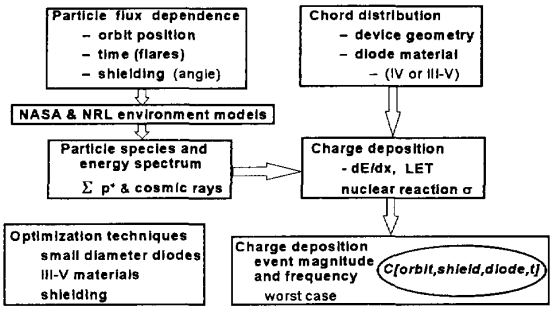

Figure 4. The frequency and amount of charge deposited in a given device depends on the orbital and satellite environment as well as the device materials, technology, and geometry.

We also consider the device specific factors such as the geometry which may in turn depend on the material, since III-V direct bandgap materials are typically much thinner than Si or Ge photodiodes. The sensitive region's geometry determines the range of possible path lengths as given by the chord length distribution. Knowing this, along with the material composition and the particle environment, enables the evaluation of charge deposition. This is done separately for each ion species, and for both direct ionization (LET) and for collisions and nuclear reactions according to the governing cross-sections.

The above treatment leads to a final result which describes the probability of encountering a given amount of charge within a certain time interval, such as a bit period. The result is dependent on the orbit position and conditions such as solar flares, the amount of spacecraft shielding, the device material, and the device size and shape. From this treatment we recognize possible approaches to minimize the frequency of events by using device structures which are as small as possible and, if necessary, by shielding. We also note that the magnitude of the larger events can be limited by using thin (direct bandgap III-V materials) which limit the number of long path lengths and reduce the overall device active volume.

Though the full characterization of the ETX-75 as shown in figure 1 has not yet been extended to other data rates, proton energies and particle types, the data of figure 2 can be used to estimate BER in a given environment. To illustrate this, we have calculated what we believe to be a reasonable "worst case" environment corresponding to a large solar flare. Using the mean composition for the King-72 flare included in the CREME model, we determine that the maximum proton flux behind 80 mil Al in a geostationary orbit would result in an integral proton flux of about 2×10^5 p/cm^2/s. Basing the estimates on the 50 degree cross-section curve of figure 2, we examine the projected BER with a power margin of 6 dB. For this case, corresponding to -21 dBm for this receiver, we anticipate a worst case BER of about 3×10^{-11}, well below the typical design objective of 10^{-9}. Note this is a crude estimate assuming all particles are incident at one angle, 50 degrees, and have a single LET corresponding to that of a 63 MeV proton. Obviously, issues such as the proton energy distribution and angle of incidence must be reassessed in light of test data showing the BER response to variables such as particle LET and data rate in order to provide more accurate estimates. Test results to quantify these variables are currently being analyzed [8].

D. Circuit Effects and Options

In order to fully understand the test results and extend these data to make accurate flight prediction we examine the effects of a given amount of deposited charge. In doing so, we consider several factors including the bandwidth of the detector and first stage amplifier, the optical signal power level, and whether the data is encoded

using a Manchester approach versus 8B/10B NRZ (no return to zero), or some other technique. Figure 5 depicts a situation in which an amount of charge is sensed following a proton strike in a detector as it receives an NRZ data stream [6,9]. Rather than edge triggered and latched data detection, the circuit makes a decision based on the power level near the midpoint of the bit. As the figure depicts, the charge pulse from the proton strike appears with a very quick rise time and then decays away according to the RC time-constant associated with the circuit front-end. Thus, the effect of the ion strike depends on the time of arrival, the RC time-constant of the circuit, and the set-up time of the first stage amplifier.

The probability of a given particle-induced signal at the critical decision interval can be evaluated by combining the probability of sensing a charge of a given magnitude with these circuit-related issues. Whether or not this results in corrupted data then depends on the relationship between the amount of ion-induced charge, the decision level, and the amount of "signal" present at the time a "0" is being transmitted. This can be evaluated using modifications to standard error probability expressions for inter-symbol interference. Note that the ion can corrupt a "0" but not a "1" as the addition of ion-induced charge when the optical signal is also present has no effect. However, preliminary evidence suggests that for large ionization events relative to the optical signal, more than one contiguous bit period may be affected.

Since a fixed amount of charge may corrupt a transmitted "0" in a manner which can be related to standard inter-symbol interference analysis, we recognize that these effects might be mitigated using the same approaches used to assure low BERs under normal conditions. For example, if a BER of 10^{-13} is required, then the link must perform with incident optical power well above the maximum sensitivity of the receiver. Similarly, as demonstrated in the data of figure 2, increased optical power can raise the receiver's threshold level to mitigate the effects of ion strikes.

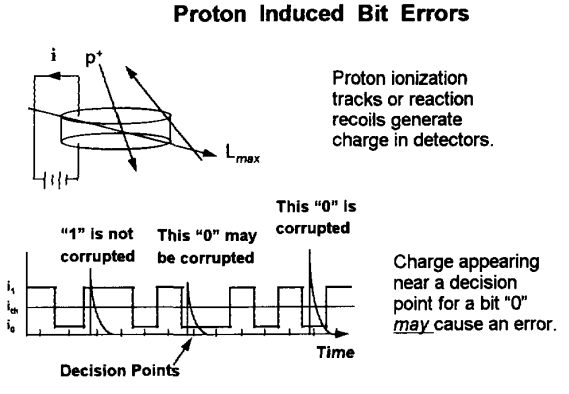

Figure 5. The effect of a given amount of charge depends on the time of arrival, the circuit parameters, the receiver design, and the amount of optical power incident.

The treatment outlined here must be modified if considering edge-triggered latched receivers or Manchester encoded data. We note that edge triggering and latching is probably not the best approach since this extends the sensitive time window to the entire bit period. Rather, it appears better to minimize the RC time constant of the amplifier front-end to minimize the sensitive time window for data corruption by ion-strikes. In addition, if the temporal characteristics of the ion-induced signal differ markedly from the optical signal, it may be possible to apply filtering approaches to reject the particle events. This approach is currently being explored for receiver designs below 100 Mbps. For Manchester encoded data, we note that it is possible to corrupt both "1"s and "0"s, though the result is a invalid code which is immediately detected, rather than a bit error.

IV. Conclusions

We report measured proton-induced bit error rates for a data link operating at 400 Mbps. Protons incident on InGaAs photodetectors disrupt link performance in a manner which depends on the particle trajectory and the optical power of the 1300 nm signal.

For bus designs requiring low error rates, we identify several optimization techniques. These include the use of III-V direct bandgap detectors such as InGaAs for 1300 nm operation, small geometry photodiode structures, bright sources to mitigate the noise-like effects of particle traversals, level sensing receiver designs, possible filtering techniques to discriminate against the particle-induced signal, and system level error detection and correction as required.

While it is not practical to exclude all particle-induced effects, we consider it possible to attain acceptable bus performance with minor constraints to the system design. As a design goal, uncorrected BERs of better than 10^{-11} seem easily attainable for point-to-point links and 10^{-9} for 32 port busses, even in severe proton environments such as the heart of the belts or during a large solar flare.

Using the approaches outlined here, in conjunction with accepted approaches for system design for radiation environments, we expect that the many advantages of fiber based data links and busses will be made available for emerging satellite requirements to transmit data reliably at rates from a few Kbps into the Gbps regime.

V. REFERENCES

1. B.S. Smith, "SEDS Segment Specification for a MIL-STD-1773 Data Bus System for the Small Explorer Data System", NASA GSFC-730-89-011 (1990)

2. C. J. Dale and P.W. Marshall, "Radiation response of 1300 nm optoelectronic components in a natural space environment", Proc. SPIE, Vol. 1791, pp. 224-232, (1992).
3. K.A. LaBel, E.G. Stassinopoulos, P. Marshall, E. Petersen, C.J. Dale, C. Crabtree, and C. Stauffer, "Proton irradiation SEU test results for the SEDS MIL-STD-1773 fiber optic data bus: integrated optoelectronics", Proc. SPIE, Vol. 1953, pp. 27-36, (1993).
4. D.C. Meshel, G.K. Lum, P.W. Marshall, and C.J. Dale, "Radiation Testing of InGaAsP Fiber Optic Transmitter and Receiver Modules," To be published in the IEEE Nuclear and Space Radiation Effects Workshop Proceedings, 1993.
5. K.M Murray, W.J. Stapor and C.Castenada, "Calibrated Charged Particle Measurement System with Precision Dosimetric Measurement and Control," Nuc. Inst and Meth., B56/57, p. 616, (1991).
6. P.W. Marshall, K.A. LaBel, C.J. Dale, J.P. Bristow, E.L. Petersen, and E.G. Stassinopoulos, "Physical Interactions Between Charged Particles and Optoelectronic Devices and the Effects on Fiber Based Data Links," Proc. SPIE, Vol. 1953, pp. 104-115, (1993).
7. Kenneth A. LaBel, Paul W. Marshall, Cheryl J. Dale, Christina M. Crabtree, E.G. Stassinopoulos, Jay T. Miller and Michele M. Gates, "SEDS MIL-STD-1773 Fiber Optic Data Bus: Proton Irradiation Test Results and Spaceflight SEU Data," IEEE Trans. on Nucl. Sci., NS-40, No. 6, pp. 1638-44, (1993).
8. Paul W. Marshall, Cheryl J. Dale, Martin A. Carts, and Kenneth A. LaBel, "Particle-Induced Bit Errors in High Performance Fiber Optic Data Links for Satellite Data Management," Submitted to the IEEE Trans. on Nucl. Sci., NS-41, No. 6, (1994).
9. Julian Bristow and John Lehman, "Component Tradeoffs and Technology Breakpoints for a 50 Mbps to 3.2 Gbps Fiber Optic Data Bus for Satellite Applications," Proc. SPIE, Vol. 1953, pp. 159-169, (1993).